International Journal for Modern Trends in Science and Technology
Volume 11, Issue 09, pages 228-238.
ISSN: 2455-3778 online
Available online at: http://www.ijmtst.com/vol11issue09.html
DOI: https://doi.org/10.5281/zenodo.18133859

Hybrid Integration of Onboard Charger and Wireless Power Transfer for EVs with Shared Coupler, Compensation, and Rectifier in a Grid-Connected Solar PV System for Optimized Fast Charging

Dr.J.Srinu Naick, M. Aishwarya, R. Surya Teja , B. Indrasena Reddy , K. Pavan Yadav, Y. Veerendra

Department of Electrical and Electronics Engineering, Chadalawada Ramanamma Engineering College, Andhra Pradesh, India.

To Cite this Article
Dr.J.Srinu Naick, M. Aishwarya, R. Surya Teja , B. Indrasena Reddy , K. Pavan Yadav & Y. Veerendra (2025). Hybrid Integration of Onboard Charger and Wireless Power Transfer for EVs with Shared Coupler, Compensation, and Rectifier in a Grid-Connected Solar PV System for Optimized Fast Charging. International Journal for Modern Trends in Science and Technology, 11(09), 228-238. https://doi.org/10.5281/zenodo.18133859

Article Info
Received: 02 September 2025; Accepted: 28 September 2025.; Published: 30 September 2025.

KEYWORDS

Electric Vehicle (EV), Bidirectional Wireless Power Transfer (BWPT), Grid Integration, Solar Charging, LCL Filter, Boost Converter, G2V, V2G, High-Frequency Magnetic Coupling, Renewable Energy

ABSTRACT

The present work proposes a new design for a high efficiency bidirectional wireless charging system for electric vehicles (EV), capable of being supplied by both solar energy and the electrical grid, to improve the operational flexibility and reliability of EV charging. In order to ensure that the two different types of energy supply can be integrated into a single system and in order to take advantage of their different characteristics, the proposed bidirectional wireless charging system consists of two separate processing paths for each type of energy source. One path processes the electrical grid power via an LCL filter and an AC-DC converter; whereas the other path uses a solar photovoltaic panel as an energy source processed through a DC-DC boost converter. These two processing paths are then fed to a bidirectional WPT unit which is able to transmit power from the grid to the EV (G2V mode) or from the EV back to the grid (V2G mode). The proposed bidirectional WPT unit makes use of high frequency magnetic coupling and phase shift control to manage the direction of energy transmission between the grid and the EV. As the proposed system is bidirectional, it can operate at low power losses, provide good power quality during wireless charging, and achieve soft switching operation due to the absence of hard switching components. Additionally, the inclusion of solar power into this system will enhance the operational reliability and resilience of the system, especially during periods when there are grid failures and will help to reduce reliance on non-renewable energy resources.

1. INTRODUCTION

The world-wide transition to sustainable transportation is generating increased interest in the rapid expansion of electric vehicles (EV). As a result, there is increasing demand for flexible, efficient, and "smart" charging infrastructure to accommodate the growth in EV. Traditional EV charging methods, such as plug-in systems and onboard chargers, generally use grid-only power. Although they are capable of providing reliable service, they suffer from significant shortcomings, including limited scalability, grid-based power outages resulting in interrupted energy delivery, and low levels of integration with renewable energy sources, such as solar energy [1], [2]. In addition, many wireless power transfer (WPT) systems are one-way; they provide only vehicle charging capabilities, and therefore do not allow for grid support through vehicle-to-grid (V2G) functionality [3], [4]. Recently developed approaches that integrate onboard chargers with wireless systems have used shared magnetic couplers and compensation networks to decrease hardware complexity. These approaches however continue to be limited in their ability to achieve dual-source adaptability and to operate continuously at varying levels of power output. Such limitations will likely be most pronounced in areas with unreliable grid access or those experiencing high peak demand periods where load shedding and blackouts are frequent occurrences. Furthermore, the inability to utilize bi-directional energy flow, limits the capability of the overall system to participate in grid balancing and energy storage during inactive time periods of EV. To mitigate the above identified shortcomings, this research develops a bi-directional WPT EV charging system that incorporates both a utility grid source and a solar PV source. The overall system architecture consists of an LCL or LC filter and AC-DC converter for grid-side power conditioning, and a solar boost converter utilizing MPPT to maximize solar energy extraction [5], [6]. The dual input provides a redundant means of delivering power and reduces dependence on non-renewable energy sources. A high frequency bidirectional wireless power transfer unit is utilized to efficiently transfer energy via magnetic coupling and soft switching. Using phase shift modulation, the unit allows for G2V and V2G operating modes, facilitating dynamic energy transfer based upon demand or availability. Through the incorporation of resonant circuits and high frequency transformers, the system achieves superior EMC performance, lower thermal losses, and higher energy conversion efficiencies than previous approaches. The elimination of the need for physical connectors, decreased maintenance costs, and increased safety, make this a suitable option for public charging station applications. Additionally, the use of electromagnetic isolation between the source and load ensures that the system maintains long term durability and safety. This dual input, bi-directional configuration, in addition to enhancing the overall system efficiency and energy reliability, will aid in meeting global objectives for sustainable, decentralized, and intelligent power systems. The system design meets relevant international standards such as IEEE Std 1547 for interconnecting distributed resources with the utility grid, IEEE Std 2030.1.1 for DC microgrids, and SAE J2954 for WPT in EVs. The system also meets IEC 61000-3-2 and IEEE 519 [7], [8] standards for power quality and harmonic distortion. Finally, due to its modular and scalable design, the system can be integrated into smart home energy management systems and microgrid environments. The inclusion of renewable energy will also contribute to the reduction of greenhouse gas emissions and increase energy independence. Considering current concerns regarding fossil fuel depletion and environmental pollution, this approach does not only promote environmentally friendly transportation but also reinforces national energy security. Therefore, the proposed system represents a forward compatible solution for modern EV charging needs, including the integration of renewable energy and smart grid interactions within a compact wireless form factor [9]. This work contributes to the continued development of future generation EV charging infrastructure through the promotion of clean energy adoption, improvements in power quality, and the assurance of uninterrupted EV charging in all operational scenarios [10], [11].

2. SYSTEM CONFIGURATION

A wireless EV charging system that utilizes grid and solar-based energy as a source of charge has been developed by using a bi-directional wireless power transfer method. The use of a bi-directional wireless

power transfer method will allow for continuous and efficient charging regardless of the availability of the grid, and support the utilization of renewable energy as well. First, the grid AC input is filtered using an LCL filter to minimize the amount of harmonic distortions and provide better power quality [13],[14]. Following filtering, a PFC AC-DC converter is used to convert the filtered AC into a DC signal, thus ensuring a high power factor and minimizing harmonic distortion as shown in Fig.1. Concurrently, a solar PV system is connected through a boost converter, and the boost converter utilizes an MPPT (Maximum Power Point Tracking) controller to ensure that the maximum amount of energy possible is being extracted from the sun at all times, independent of changing sunlight levels. The output of each of the two sources are connected to a single, high-voltage DC bus. The DC bus serves as the supply of power to the bi-directional wireless power transfer system. The bi-directional wireless power transfer system consists of a high frequency inverter on the transmitter side and a rectifier on the receiver side. The loosely coupled coils located on the transmitter and receiver sides of the system are used to transfer power wirelessly, and phase shift modulation is used to provide soft switching and maximize efficiency. The system provides the capability to charge or discharge an EV, supporting both G2V (Grid to Vehicle) and V2G (Vehicle to Grid), providing the ability to send energy to the grid when it is needed [11],[12]. The DC power supplied to the EV charger is utilized to charge the EV battery using constant current and constant voltage control methods. The operation of the converters and communication protocols are monitored and controlled in real time using a digital controller that monitors the overall performance of the system, including the protection of the system and its interaction with the grid and the battery management unit.

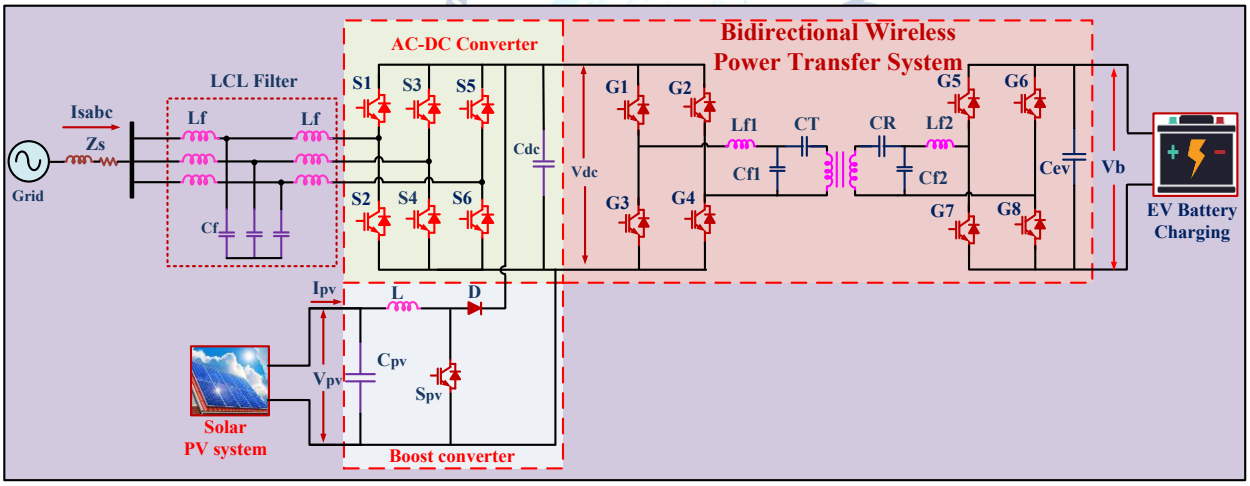

Fig.1 proposed system configuration

3. MODELING AND DESIGNING OF PROPOSED SYSTEM CONFIGURATION

A. Solar PV system

A simple diode model that shows how a solar cell performs in different environments, including variations in temperature and solar radiation. When light from the sun hits the solar cell, it produces a photocurrent Iph, which will increase proportionately with an increase in the level of solar radiation but will vary slightly with temperature. The diode portion of the model describes the p-n junction within the solar cell and accounts for the loss of electrons due to recombination, and the series resistor Rs accounts for internal resistive losses in the solar cell as shown in Fig.2. The shunt resistor Rsh describes leakage currents in the solar cell. The output current I is described as the difference between the photo-generated current and the current lost to the diode due to reverse-biasing, with adjustments made for voltage drops across resistors. This relationship is nonlinear, and so typically must be solved iteratively for simulations and designs to be accurate. The solar cell operates differently depending on the applied operating voltage V. At open circuit, the current produced is zero volts; at short circuit, the voltage is zero amps. Between these extremes is the maximum power point (MPP) where the product of the current and voltage (i.e.,

power) are greatest, representing the most efficient operating point for the PV cell. In practice, MPPT algorithms (such as incremental conductance and perturb & observe) continuously adjust the operating point of the load or the duty cycle of the converter in response to changes in solar radiation and/or temperature to maintain operation at the MPP. This maximizes the amount of energy collected. The single diode model provides a reliable and widely used framework for the analysis, simulation and design of PV systems and allows engineers to accurately predict the performance of PV systems under various environmental conditions and to optimize the performance of system components such as DC-DC converters and energy storage devices.

a. Single Diode Model of a PV Cell

The single diode model is widely used to represent the electrical behavior of a solar cell or PV module, capturing its nonlinear current-voltage (I-V) characteristics.

1. Equivalent Circuit: A current source Iph in parallel with a diode (with saturation current I0), series resistance Rs, and shunt resistance Rsh.

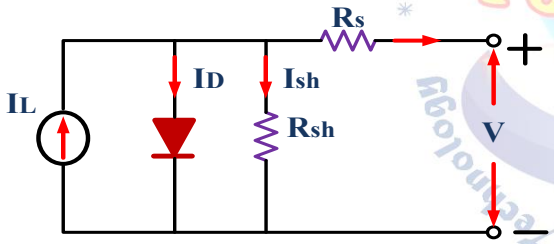

Fig. 2 equivalent model of PV solar.

2. Output Current Equation:

$$I_{ph} - I_0\left(e^{\frac{q(V+IR_S)}{nkT}-1}\right) - \frac{V+IR_S}{R_{sh}} \qquad (1)$$

Where:

- I = output current (A)
- V = output voltage (V)
- Iph = photo-generated current (A)
- I0 = diode saturation current (A)
- q = electron charge 1.602×10−19 C)
- n = diode ideality factor (typically 1 to 2)
- k = Boltzmann constant 1.381×10−23 J/K
- T = cell temperature (Kelvin)
- Rs = series resistance (Ω)
- Rsh = shunt resistance (Ω)

3. Photo-generated current Iph:

$$= \left[I_{sc} + K_i(T - T_{ref})\right] \times \frac{G}{G_{ref}} \qquad (2)$$

Where:

- Isc = short-circuit current at reference temperature
- Ki = temperature coefficient of current (A/°C)
- Tref = reference temperature (usually 25°C or 298 K)
- G = solar irradiance (W/m²)
- Gref = reference irradiance (1000 W/m²)

4. Diode Saturation Current I0:

$$I_0 = I_{0_{ref}}\left(\frac{T}{T_{ref}}\right)^3 \exp\left(\frac{qE_g}{nk}\left(\frac{1}{T_{ref}} - \frac{1}{T}\right)\right) \qquad (3)$$

Where:

- I0ref = diode saturation current at Tref
- Eg = bandgap energy of the semiconductor (eV)

5. Open-circuit voltage Voc:

$$V_{oc} = \frac{nkT}{q} In\left(\frac{I_{ph}}{I_0} + 1\right) \qquad (4)$$

B. Solar PV boost Converter

A boost converter is a DC-DC converter that boosts a lower input DC voltage to a higher output DC voltage, as depicted by Fig. 3. The primary components include a switch (typically a MOSFET), a diode (D), an inductor (L), and a DC output capacitor (C). When the MOSFET switch is turned ON, it closes, which allows current to flow from the PV panel through the inductor. The stored energy is placed in the magnetic field of the inductor when the diode remains reverse-biased and does not allow current to reach the output as shown in Fig.3. Once the MOSFET is turned OFF, the magnetic field of the inductor collapses and releases the stored energy. At this time, the current of the inductor flows from the diode to the output capacitor and to the load; thereby increasing the input voltage. As a result, the output voltage will be greater than the input voltage; thus efficiently providing a voltage increase suitable for charging batteries or supplying power to loads.

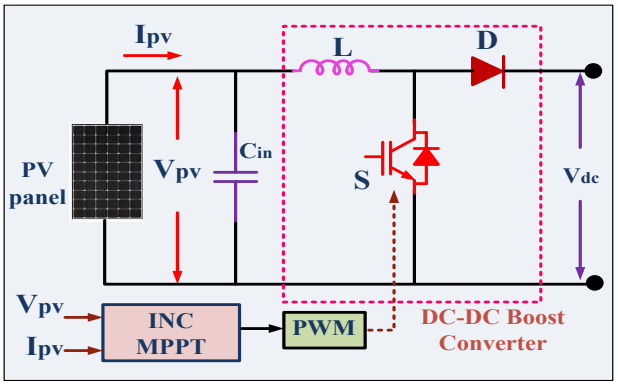

Fig. 3 solar PV INC MPPT DC-DC boost converter

1. Output Voltage of Boost Converter

$$V_o = \frac{V_{in}}{1-D} \quad (5)$$

Where: Vo: Output voltage, Vin: PV input voltage, D: Duty cycle (0 < D < 1)

2. Inductor Value (L)

$$L = \frac{V_{in} \cdot D}{f_S \cdot \Delta I_L} \quad (6)$$

Where:

- fs: Switching frequency (Hz)
- ΔIL: Inductor ripple current (A), usually 20–40% of Iin

3. Output Capacitor Value (C)

$$C = \frac{I_O \cdot D}{f_S \cdot \Delta V_O} \quad (7)$$

Where:

- Io: Output current (A)
- ΔVo: Acceptable output voltage ripple (V)

C. MPPT Control

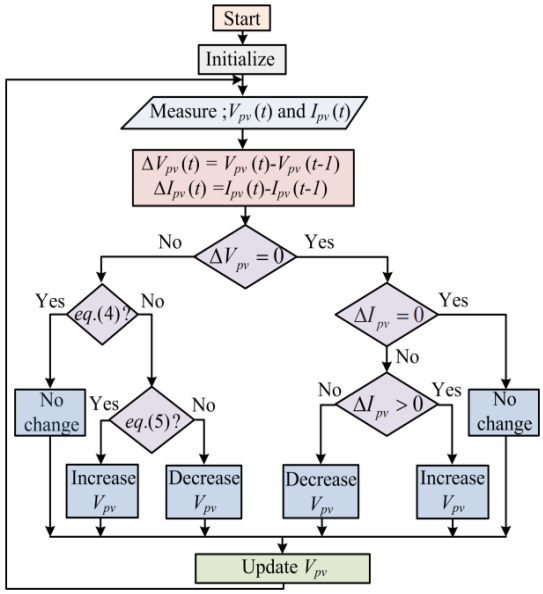

Fig. 4. INC MPPT control

Fig. 4 depicts the solar PV array's greatest power point technique. It generates a voltage reference (V*pv) that is the same as the MPP voltage of the PV array.

At the MPP,

$$\frac{dP_{PV}}{dV_{PV}} = 0 \quad (8)$$

$$\frac{d(V_{PV}I_{PV})}{dV_{PV}} = I_{PV} + V_{PV}\frac{dI_{PV}}{dV_{PV}} = 0 \quad (9)$$

$$\frac{dI_{PV}}{dV_{PV}} = -\frac{I_{PV}}{V_{PV}} \quad (10)$$

Right side displays PV array instantaneous conductance. Conditions of INC MPPT control:

$$\frac{dI_{PV}}{dV_{PV}} = -\frac{I_{PV}}{V_{PV}}\left(\frac{dP_{PV}}{dV_{PV}} = 0, \text{at MPP}\right) \quad (11)$$

$$\frac{dI_{PV}}{dV_{PV}} > -\frac{I_{PV}}{V_{PV}}\left(\frac{dP_{PV}}{dV_{PVg}} > 0, \text{at left of MPP}\right) \quad (12)$$

$$\frac{dI_{PV}}{dV_{PV}} < -\frac{I_{PV}}{V_{PV}}\left(\frac{dP_{PV}}{dV_{PV}} < 0, \textit{at right of MPP}\right) \quad (13)$$

According to the circumstances, the disturbance arises in the PV array's voltage, which is used to monitor the array's maximum power point.

4. DESIGNING OF THE BWPT SYSTEM

The BWPT System is designed around the development of a Phase Shift Controller to provide Power Factor Correction (PFC) and to Optimize the Efficiency of Power Transferred Between Primary and Secondary Coils at the Resonance Frequency as depicted in Figure 7. The efficiency of the Power Transfer is dependent upon Mutual Inductance (M), which can be influenced by Coil Size, Turns, Air Gap and Coil Coupling Coefficient (K). Higher Coil Coupling Coefficients (K) can be obtained by increasing Pad Diameter and decreasing Air Gap, Ferrite Core use further enhances Coil Coupling Coefficients (K). The system will operate at 85kHz and follow the SAE J2954 Standard for Wireless Charging Systems. The system will incorporate LCC-LCC Compensation Circuits for the Primary and Secondary Coils to provide additional flexibility in controlling Coil Currents and Voltage Levels as shown in Fig.5. Coil Currents are directly related to the Compensating Inductances, which must be carefully chosen to reduce Coil Current while avoiding Increased Coil Voltage Levels which may negatively affect Safety and Reliability. Relationships between Coil Voltage and Coil Current are defined using Equations for Coil Turns, Inductance Per Turn, and the Compensating Inductor Values. Following the determination of Coil Design, Capacitor Values for the Resonant Circuit are determined using the Resonance Frequency to maximize

the performance of the system. Additionally, the design includes Electrical, Magnetic, and Thermal Factors such as the Width of the Ferrite Core and Specifications for the Litz Wire to avoid Excessive Losses in the Ferrite Core and Maintain Component Integrity. Lastly, Voltages and Currents in the Components of the Resonant Tank are Calculated to Meet Operational Requirements While Considering Heating and Safety Constraints of High-Frequency and High-Power Capacitors.

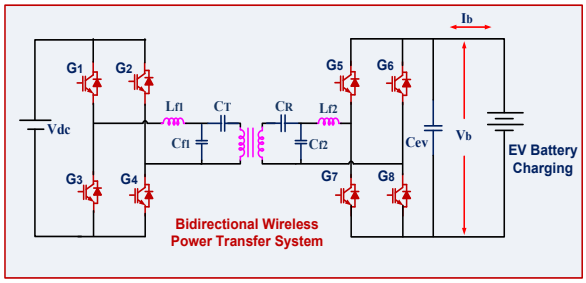

Fig.5 Bidirectional Wireless Power Transfer for EV charging system

The design of the Bidirectional Wireless Power Transfer(BWPT) system focuses on efficient power transfer between the primary and secondary coils at the resonance frequency, which can be expressed as:

$$P = \omega_0 M I_p I_s \quad (14)$$

where ω0 is the angular resonance frequency, M is the mutual inductance between the coils, and Ip, Is are the RMS currents in the primary and secondary coils, respectively. The mutual inductance M depends on the coupling coefficient K and the self-inductances of the coils:

$$M = K\sqrt{L_p L_s} \quad (15)$$

Here, Lp and Ls are the self-inductances of the primary and secondary coils, and K is influenced by coil size, spacing (air gap), and the presence of ferrite cores which improve coupling by 30%-50%. The output power is also given by:

$$P = 2\pi f_0 (N_p I_p)(N_s I_s) K \sqrt{\hat{L}_p \hat{L}_s} \quad (16)$$

where f0 is the operating frequency (85 kHz), Np and Ns are the number of turns in primary and secondary coils, and L^p, L^s are inductances per turn.

Using LCC-LCC compensation circuits enhances system control and efficiency. The coil currents relate to input voltages VAB and compensating inductors L11, L22 as:

$$I_p = \frac{V_{AB}}{\omega_0 L_{11}}, \; I_s = \frac{V_{ab}}{\omega_0 L_{22}} \quad (17)$$

Adjusting L11 can reduce primary coil current, but increasing coil turns also raises coil inductance and voltage, limited by insulation and safety constraints. Coil voltages are calculated by:

$$V_{L_p} = I_p X_{L_p} = j\omega L_p I_p = I_P (2\pi N_p^2 \hat{L}_p) \quad (18)$$

$$V_{L_s} = I_s X_{L_s} = j\omega L_s I_s = I_s (2\pi N_s^2 \hat{L}_s) \quad (19)$$

The voltage gain ratio between coil voltage and input voltage is:

$$G_{vp} = \frac{V_{Lp}}{V_{AB}} = \frac{X_{Lp}}{X_{L_{11}}} = \frac{L_p}{L_{11}} \quad (20)$$

The resonance frequencies for the LCC compensation tanks are given by:

$$\omega_0 = \frac{1}{\sqrt{L_{11} C_{11}}} = \frac{1}{\sqrt{(L_p - L_{11}) C_{12}}} \quad (21)$$

$$\omega_0 = \frac{1}{\sqrt{L_{22} C_{22}}} = \frac{1}{\sqrt{(L_S - L_{22}) C_{21}}} \quad (22)$$

Currents through the resonant tank's tuning inductors and coils are:

$$I_{L_{11}} = \frac{M V_{AB}}{\omega_0 L_{11} L_{12}} \quad (23)$$

$$I_{L_{22}} = \frac{M V_{ab}}{\omega_0 L_{11} L_{22}} \quad (24)$$

$$I_{L_p} = \frac{V_{AB}}{\omega_0 L_{11}} \quad (25)$$

$$I_{L_s} = \frac{V_{ab}}{\omega_0 L_{22}} \quad (26)$$

Voltages across the tuning capacitors are:

$$V_{C_{12}} = V_{AB} \frac{(L_p - L_{11})}{L_{11}} \quad (27)$$

$$V_{C_{21}} = V_{ab} \frac{(L_S - L_{22})}{L_{22}} \quad (28)$$

The design involves balancing coil turns, inductance, and compensation capacitances to ensure efficient power transfer, stable resonance, and adherence to voltage and current limits imposed by the components and safety requirements.

5. CONTROL ALGORITHM

The proposed system has been developed for the highest output of 10kW with rated voltage for Solar Photovoltaic (SPV) Bidirectional DC-DC Charging Station. The SPV array was designed and installed in order to supply the Electric Vehicle (EV) loads while operating under this mode. On the charging station, an additional 10 kW SPV array is installed for supplying to the EV battery for residential, home, office and public charging applications. V2V Mode: In B2V mode; both charging and discharging processes will take place at the same time. Therefore, for successful implementation of the Single Phase Shift Current Control Algorithm is utilized as shown in Fig.6. The mathematical representation of the controller can be described as:

Modeling of the Controller:

The battery current error is given as:

$$I_b^*(t) - I_{b1}(t) = e(t) \quad (29)$$

Where Ib*(t) is reference value of battery current, Ib1(t) is the main battery current and e(t) is the error signal generated. This error signal is passed through PI controller whose transfer function is given as:

$$K_p + \frac{K_i}{s}$$

$$e(t) \times K_P + e(t) \times \frac{K_i}{s} = u(a) \quad (30)$$

For proper designed value of Ki and Kp, an output signal is generated, which is multiplied by the constant α. Where α is taken as,

$$\alpha = 0.5 \times \frac{1}{3200} \quad (31)$$

Where $\frac{1}{32000}$ is the switching time period

The output of equation (31), represents a variable time delay in relation to the first bridge of the converter (as shown in Fig.6). The time delay has values from 4µs to 5µs and thus the time delay dictates the power that will be delivered at the output of the system. The charging and discharging control strategy are presented in Fig. 8 and Fig.7 respectively. The timing of the switching for charging and discharging are illustrated in the switching waveforms in Fig.8.

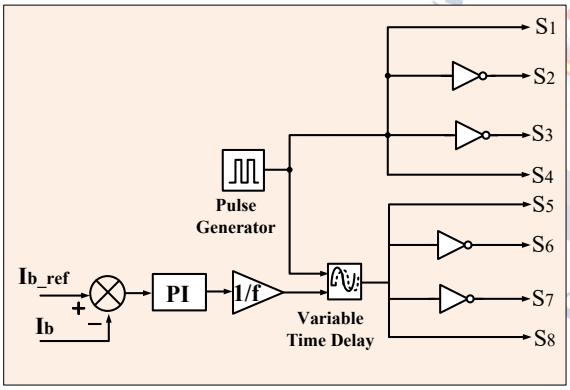

Fig.6 DAB charging algorithm

Discharging Mode:

For the discharging mode the similar technique is used. The reference current is added to the auxiliary battery current and

$$I_b^*(t) - I_{b2}(t) = e_a(t) \quad (32)$$

Switching pulse is also reversed in order to reverse the power flow. The mathematical formulation of discharging controller is given as,

$$e_b(t) \times K_p + e_b(t) \times \frac{K_i}{s} = u(b) \quad (33)$$

The u(b) signal is again multiplied with the constant value α and generated u(ref2), where α value is taken as:

$$\alpha = 0.5 \times \frac{1}{32000} \quad (34)$$

Where $\frac{1}{3200}$ is the switching time period now u (ref2) is acting as a delay to the primary bridge of the DAB converter with respect to the secondary bridge of converter and hence power is now transferred from secondary bridge side to primary bridge side

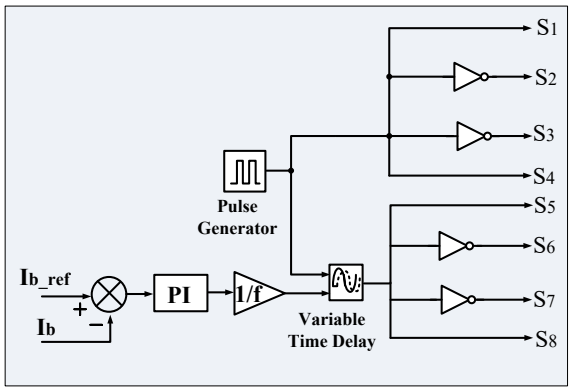

Fig.7 DAB discharging algorithm

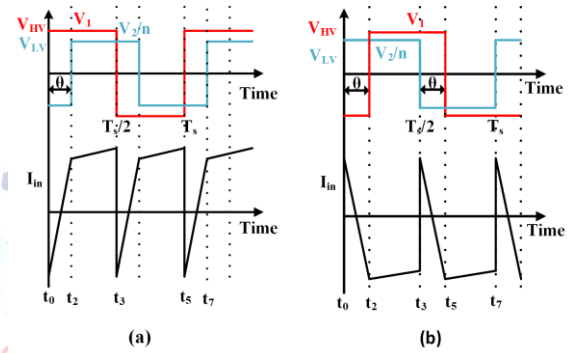

Fig. 8 (a)Voltage and input current waveforms in forward power flow; (b)Voltage and input current waveforms in reverse power flow

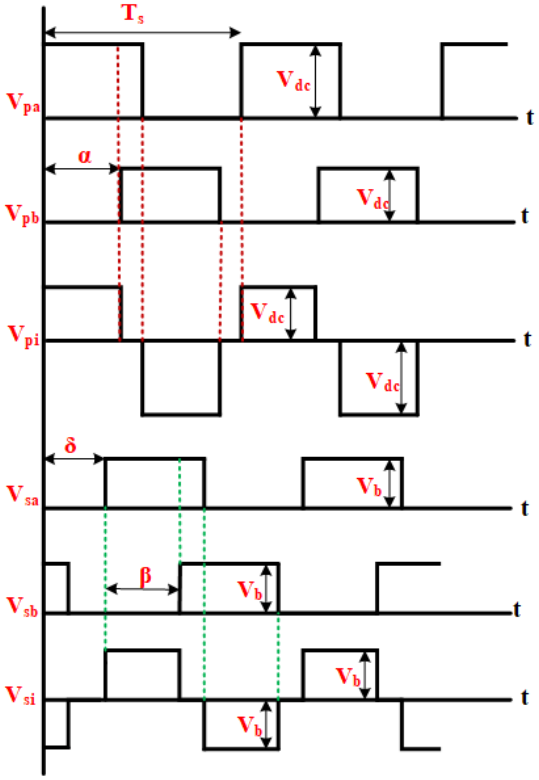

Fig 9. Switching waveforms of phase angle delay between the two converters.

6. MODELLING AND DESIGNING OF BATTERY ENERGY STORAGE SYSTEM

In hybrid network systems, the Battery Energy Storage System (BESS) has a critical role to play in managing energy, stabilizing the grid, and improving power quality. When connected to the grid, it utilizes a bi-directional DC-DC Converter as its interface, with common configurations being either Buck-Boost or Bidirectional Half-Bridge topologies that control both the charging and discharging of the BESS. While maintaining a constant DC Bus Voltage level, the converter will adjust the direction of power flow depending on grid needs (i.e., high demand), generation surpluses (e.g., when solar or wind production exceeds current consumption), or loading requirements.

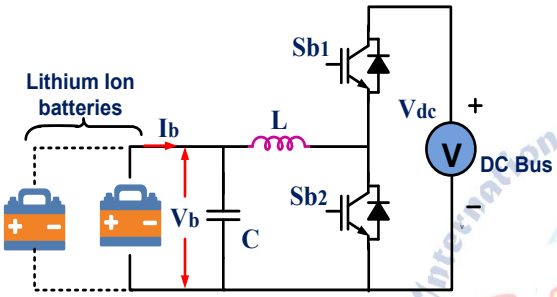

Fig.10 principle operation bidirectional dc-dc buck boost converter

The direction of power flow is controlled by measuring the state of charge (SOC), voltage, and current of the battery in real time. The charging power Pch and discharging power Pdis are defined as:

$$P_{\text{ch}} = V_b \cdot I_{\text{ch}} \quad (35)$$

$$P_{dis} = V_b \cdot I_{dis} \quad (36)$$

where Vb is the battery voltage, Ich is the charging current (positive into battery), and Idis is the discharging current (positive out of battery). The control strategy ensures that the SOC remains within safe limits, typically between 20% and 90%, to avoid overcharging or deep discharge. The SOC is estimated using the Coulomb counting method:

$$SOC(t) = SOC(t_0) - \frac{1}{C_{bat}} \int_{t_0}^{t} I_{bat}(\tau)\, d\tau \quad (37)$$

Where Cbat is the nominal capacity of the battery and Ibat is the battery current (positive when discharging) in the second case, the Double Loop Control Strategy is used in Advanced Battery Energy Storage System (BESS), particularly in Hybrid Renewable Systems, to achieve stable regulation of the battery's power flow and maintain the DC-Link Voltage Stability. This Double Loop Controller has two nested loops: the Outer Voltage Control Loop and the Inner Current Control Loop. The Outer Voltage Loop maintains the DC-Link Voltage Vdc at the reference value Vdc∗, thus controlling Power Exchange with the Grid and/or Connected Loads as shown in Fig.11. The error between the Reference DC-Voltage Vdc∗ and the Actual DC-Voltage Vdc is calculated by the PI Controller, that calculates the reference Battery Current Ibat∗ for the Inner Loop:

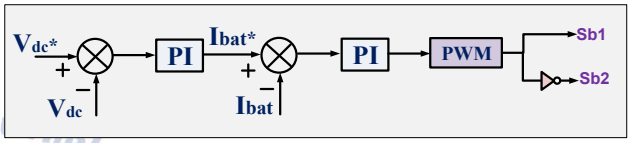

Fig. 11 double loop ev charging controller

$$I^*_{bat} = K_{pv}(V^*_{dc} - V_{dc}) + K_{iv} \int (V^*_{dc} - V_{dc})dt \quad (38)$$

Here, Kpv and Kiv are the proportional and integral gains of the outer voltage loop.

The inner current loop then tracks this reference battery current Ibat∗. The actual battery current Ibat is compared with the reference, and the error is fed to another PI controller, which generates the control voltage signal Vbat∗ used to adjust the duty cycle D of the bidirectional converter:

$$V^*_{bat} = K_{pi}(I^*_{bat} - I_{bat}) + K_{ii} \int (I^*_{bat} - I_{bat})\, dt \quad (39)$$

Where Kpi and Kii are the proportional and integral gains of the inner current loop.

This output voltage Vbat∗ is then modulated using PWM (Pulse Width Modulation) to control the converter's switching, allowing power to flow into (charging) or out of (discharging) the battery.

7. RESULTS AND DISCUSSION

A Bidirectional Wireless Electric Vehicle Charging System is designed for use as a Smart Grid and Renewable Energy Source. To analyze the Bidirectional Wireless Electric Vehicle Charging System's performance under a variety of operational modes, A

bidirectional wireless electric vehicle charging system was modeled and simulated using MATLAB/Simulink. The system was tested for both grid and solar inputs to demonstrate its capability to provide continuous and reliable charging. Results from the simulations indicated that the AC/DC Converter with Power Factor Correction (PFC), which synchronized the input current of the converter to the grid voltage to achieve a nearly unity power factor and thus minimize harmonic distortion while meeting the requirements of IEEE Standard 519 for Power Quality as shown in Fig.12. The Solar Boost Converter utilizing Maximum Power Point Tracking (MPPT) control, continuously optimized the extraction of energy from the solar panels as the irradiance levels changed. These two different sources of energy were used together in the same system to prove the success of the Dual-Source Architecture because the system remained active as long as one of the two input sources was available. The Bidirectional Wireless Power Transfer (WPT) System utilized phase-shift modulation to enable soft-switching and thus reduce the stress on the switches of the system and improve overall reliability of the system; and provided an efficient means of transferring energy between loosely coupled coils with minimal loss of energy. The system was capable of providing a constant current (CC) or constant voltage (CV) charge profile to the vehicle's battery during G2V charging. Additionally, the system was capable of transitioning smoothly between CC and CV charging modes and maintaining tight control over the output of the system. Finally, the system was capable of functioning in V2G mode during simulation, where energy could be drawn from the vehicle's battery and returned to the grid under controlled conditions. Thus, the proposed system has the potential to be integrated into Smart Grid systems of the future. Overall, the simulation results demonstrated that the proposed Bidirectional Wireless Electric Vehicle Charging System is capable of providing a reliable, efficient, and bidirectional method of wireless electric vehicle charging utilizing a hybrid source of grid and solar energy; and that the proposed architecture enhances the reliability of the system, improves the quality of the power, and increases the utilization of renewable energy.

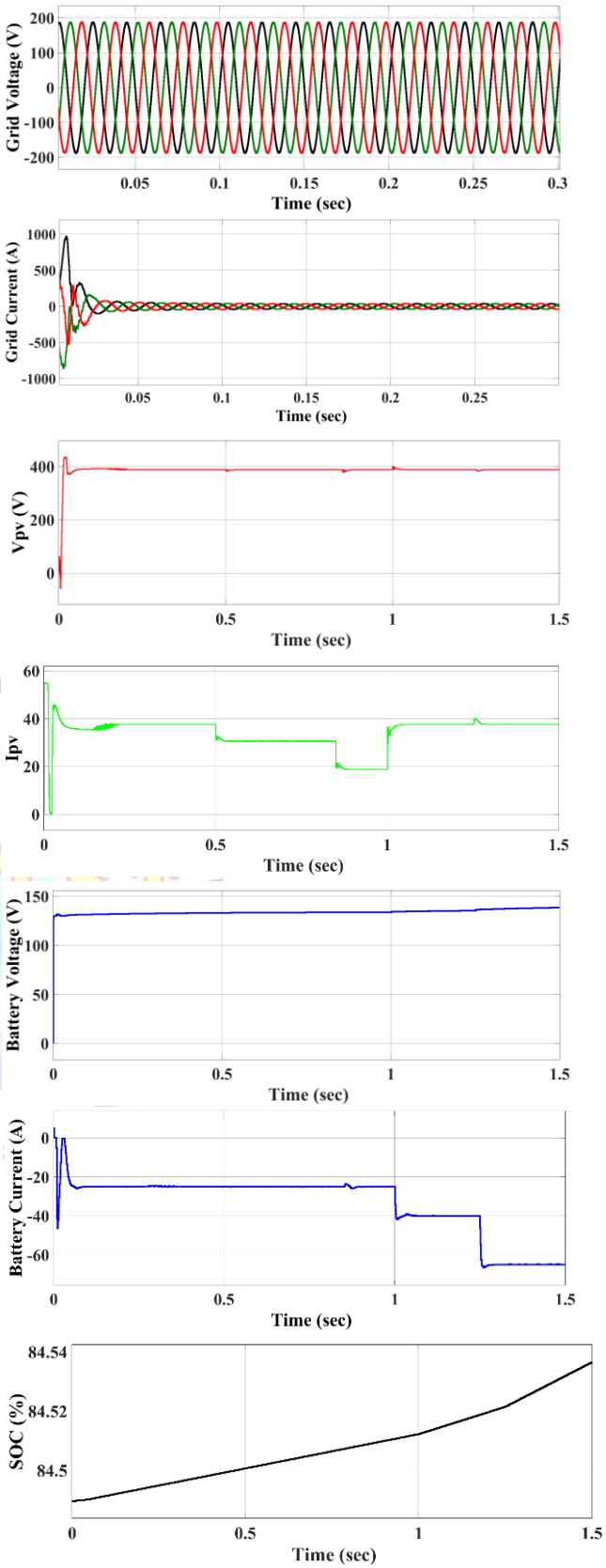

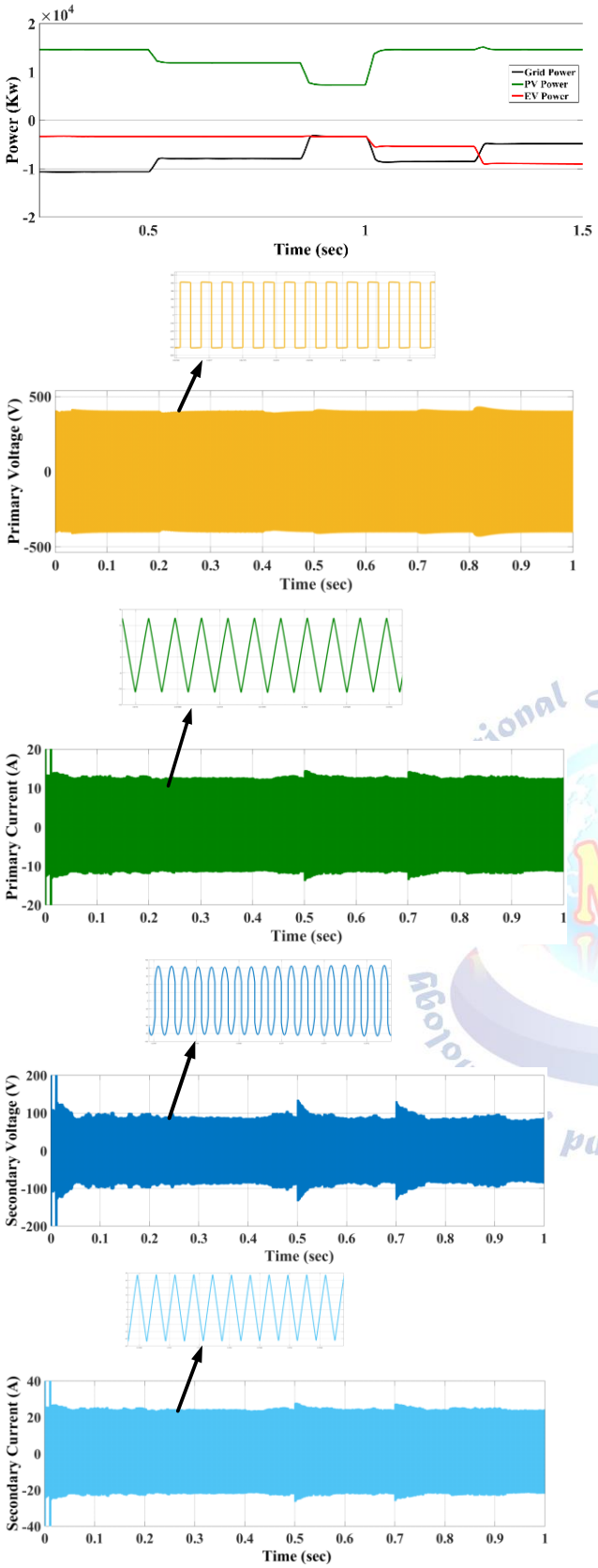

Fig.12 Simulation results of the Hybrid Solar-Battery Bidirectional Wireless Power Transfer System for EV Charging under Variable Irradiance Conditions

8. CONCLUSION

The study presents a new, bi-directional WEC system for electric vehicles that can be charged wirelessly from a combination of solar panels and the electrical grid utilizing a single, hybrid converter and a magnetic coupler. The new structure provided an answer to some of the major issues related to traditional wired and one-way EV charging systems like; lack of flexibility, limited ability to scale up, and dependency upon a single type of energy. The simulation results show that the proposed system is able to function at a high level of efficiency in both G2V and V2G operation modes. Additionally, the use of MPPT to track the MPP with the use of solar energy allowed for increased use of renewable energy sources. Finally, since grid power was used as the backup, it also ensured that there would always be sufficient energy available to charge the battery when solar power was not available. The WPT link was used to allow for a contactless method of transferring energy that has many advantages including; high efficiency, low maintenance, and higher safety levels. Lastly, the inclusion of PFC and soft-switching technologies to ensure that the power delivered to the load is of a good quality and does not cause undue stress on the switching devices. The use of a single shared converter and a bi-directional control allowed for a very compact and efficient system design allowing for the possibility of the system to recover excess energy back into the grid as well as allow for smooth transitions between the different operating modes of the system. Thus, the proposed system will make it possible to provide flexible and reliable EV charging infrastructure and promote the integration of renewable energy and support the development of future energy sharing systems. Future research could include the development of a hardware prototype and the optimization of the system for real time environmental conditions.

Conflict of interest statement

Authors declare that they do not have any conflict of interest.

REFERENCES

[1] I. Kougioulis, A. Pal, P. Wheeler, and M. R. Ahmed, "An isolated multiport DC–DC converter for integrated electric vehicle on-board charger," IEEE J. Emerg. Sel. Topics Power Electron., vol. 11, no. 4, pp. 4178–4198, Aug. 2023.

[2] H. Qari, S. Khosrogorji, and H. Torkaman, "Optimal sizing of hybrid WT/PV/diesel generator/battery system using MINLP method for a region in Kerman," Scientia Iranica, vol. 27, no. 6, pp. 3066–3074, 2020.

[3] H. Heydari-Doostabad and T. O'Donnell, "A wide-range high-voltagegain bidirectional DC–DC converter for V2G and G2 V hybrid EV charger," IEEE Trans. Ind. Electron., vol. 69, no. 5, pp. 4718–4729, May 2022.

[4] M. A. H. Rafi and J. Bauman, "Optimal control of semi-dual active bridge DC/DC converter with wide voltage gain in a fast-charging station with battery energy storage," IEEE Trans. Transport. Electrific., vol. 8, no. 3, pp. 3164–3176, Sep. 2022.

[5] X. Qu, H. Chu, S.-C. Wong, and C. K. Tse, ''An IPT battery charger with near unity power factor and load-independent constant output combating design constraints of input voltage and transformer parameters,'' IEEE Trans. Power Electron., vol. 34, no. 8, pp. 7719–7727, Aug. 2019.

[6] X. Liu, N. Jin, X. Yang, K. Hashmi, D. Ma, and H. Tang, ''A novel singleswitch phase controlled wireless power transfer system,'' Electronics, vol. 7, no. 11, p. 281, Oct. 2018.

[7] K. V. Suhaskrishnan, V. Sruthy, and P. K. Preetha, "Smart grid compatible universal electric vehicle charging outlet to boost India's EV penetration rate," in Proc. IEEE 19th India Council Int. Conf., 2022, pp. 1–6.

[8] Limits for Harmonics Current Emissions (Equipment Current 16A Per Phase), IEC Standard IEC 61000-3-2, 2000.

[9] R. Bosshard, J. W. Kolar, J. Mühlethaler, I. Stevanovic, B. Wunsch, and F. Canales, ''Modeling and η–α -Pareto optimization of inductive power transfer coils for electric vehicles,'' IEEE J. Emerg. Sel. Topics Power Electron., vol. 3, no. 1, pp. 50–64, Mar. 2015.

[10] R. Bosshard and J. W. Kolar, ''Inductive power transfer for electric vehicle charging: Technical challenges and tradeoffs,'' IEEE Power Electron. Mag., vol. 3, no. 3, pp. 22–30, Sep. 2016.

[11] V. Shevchenko, O. Husev, R. Strzelecki, B. Pakhaliuk, N. Poliakov, and N. Strzelecka, ''Compensation topologies in IPT systems: Standards, requirements, classification, analysis, comparison and application,'' IEEE Access, vol. 7, pp. 120559–120580, 2019.

[12] D. Xu, C. Zhao, and H. Fan, ''A PWM plus phase-shift control bidirectional DC–DC converter,'' IEEE Trans. Power Electron., vol. 19, no. 3, pp. 666–675, May 2004.

[13] M. Mohammad, O. C. Onar, G.-J. Su, J. Pries, V. P. Galigekere, S. Anwar, E. Asa, J. Wilkins, R. Wiles, C. P. White, and L. E. Seiber, ''Bidirectional LCC–LCC-compensated 20-kW wireless power transfer system for medium-duty vehicle charging,'' IEEE Trans. Transport Electrific., vol. 7, no. 3, pp. 1205–1218, Sep. 2021, doi: 10.1109/TTE.2021.3049138.

[14] S. A. Gorji, H. G. Sahebi, M. Ektesabi, and A. B. Rad, ''Topologies and control schemes of bidirectional DC–DC power converters: An overview,'' IEEE Access, vol. 7, pp. 117997–118019, 2019.